

We are IntechOpen, the world's leading publisher of Open Access books Built by scientists, for scientists

4,800

Open access books available

122,000

International authors and editors

135M

Downloads

Our authors are among the

154

Countries delivered to

TOP 1%

most cited scientists

12.2%

Contributors from top 500 universities



WEB OF SCIENCE™

Selection of our books indexed in the Book Citation Index
in Web of Science™ Core Collection (BKCI)

Interested in publishing with us?
Contact book.department@intechopen.com

Numbers displayed above are based on latest data collected.
For more information visit www.intechopen.com



Local Electric Fields in Dielectric and Semiconductors

Dmitry E. Milovzorov

Additional information is available at the end of the chapter

<http://dx.doi.org/10.5772/intechopen.74310>

Abstract

Local electric fields are appeared in dielectric and semiconductors due to the destruction of symmetry, creating the vacancies, point defects and chemical impurities in material. By increasing in external electric field value there are numerous structural changes will be generated. Point defects in silicon films were characterized by using electron-paramagnetic resonance spectroscopy and laser picoseconds spectroscopy. Chemical bonding properties was investigated by means of Fourier-transformed infrared spectroscopy. The possible mechanism of phase destruction was proposed.

Keywords: local field, point defect, dangling bonds, Raman spectroscopy, nanocrystals, second-harmonic generation, silicon films

1. Introduction

Local electric fields are appeared in dielectric and semiconductors due to the destruction of symmetry, creating the vacancies, point defects and chemical impurities in material. By increasing in external electric field value there are numerous structural changes will be generated. Some of them will produce such great local fields that will destroy all material or change its physical properties. The studying the nature of local electric fields will open new tendency in electronic device producing, from one side, and, help to change materials' properties according to our needs, from another side.

Description of local electromagnetic fields is a continuously durable through the all history of physics and was began with publication of first articles written by Maxwell Garnett which were devoted to colors in metal glasses and metallic films [1], Lorentz [2], and later in works of Brugeman [3] was developed by Edmund Stoner from University of Leeds [4] and Osborn

from Naval Research Laboratory [5]. For a complicated medium such as the binary system with components A and B the dielectric function can be estimated as following [5]:

$$\varepsilon = \varepsilon_a \left[1 + 2C_A \left(\frac{\varepsilon_a - \varepsilon_b}{\varepsilon_a + 2\varepsilon_b} \right) \right] \left[1 - C_A \left(\frac{\varepsilon_a - \varepsilon_b}{\varepsilon_a + 2\varepsilon_b} \right) \right]^{-1} \quad (1)$$

In a case that one component is included in another dielectric component and polarized media with averaged value of polarizability of $\langle \alpha(w) \rangle = \frac{\varepsilon_A(w) - \varepsilon_B(w)}{\varepsilon_A(w) + 2\varepsilon_B(w)}$ the Maxwell-Garnet formula is given by $\varepsilon(w) = \varepsilon_B(w) \left[1 + 2C_A \left(\frac{\varepsilon_A(w) - \varepsilon_B(w)}{\varepsilon_A(w) + 2\varepsilon_B(w)} \right) \right] \left[1 - C_A \left(\frac{\varepsilon_A(w) - \varepsilon_B(w)}{\varepsilon_A(w) + 2\varepsilon_B(w)} \right) \right]^{-1}$.

Structural properties of material may be strictly different as for surface and thin films, as for nanostructures such as clusters or nanocrystals, as for bulk material. However, it is obviously that most amounts of media in the universe is nanostructured or even in nanocrystal phase. For example, interplanetary dust was observed charged coupled devices (CCD) detectors and infrared space telescope [6]. They observed a cometary coma of Hale-Bopp comet. The dust destruction in space (Cygnus Loop supernova) was observed by using a Spitzer Telescope tuned in infrared (IR) range from 22 to 36 μm [7] and shows us the chemical properties, such as dust chemical compositions. These observations show the great fraction of silicon in all space dust. Space dust destruction and ion formation was studied by Mann and Czechovsky [8], which results from model calculations in silicate grains, carbon and ice grains. Grain destruction in a supernova remnant shock wave was investigated by astronomers of Harvard University [9]. It was observed by Spitzer telescope in IR 24 μm range of wave length. The case of impact of nanoscopic dust grain with solar wind of spacecraft already was estimated by using the dimensionless parameter equals to ratio between Debye length and radius of dust cloud spherical shell with radius R [10]. It was shown that the dust particle with mass 10^{-20} kg produces by impact 10^7 charged particles.

From the other physical scientific trends we have an observations of local field by a nonlinear spectroscopic experiments with nonmaterial and nanocomposites, particularly, semiconductors. By using semiconductor materials have been made numerous types of devices, such as electronic devices and photon detectors, integrated circuits and thin film transistors, optoelectronic devices and others. Every time when the device is developed the problem of reproducibility of its work regimes and durability of their realization is appeared. The solution of this problem is very important for device manufacturing, and it depends on properties of used active semiconductor materials. The electrical properties often are not so transparent due to slightly nonlinear behavior of their characteristics. **Figure 1** shows the current-voltage and resistance-voltage characteristics for two silicon films prepared by plasma-enhanced chemical vapor deposition technique with gas mixture of silane diluted by hydrogen and silicon tetra fluoride gas: amorphous and nanocrystallized [11]. It is seen, than their current-voltage characteristics are similar in this voltage range, but resistance-voltage characteristics are strictly different. Such difference can be explained by the disorder of amorphous phase and generating of numerous point defects by applying external electrical field. It is clear, that the voltage is varied in the range from the -10 to 10 V. Hydrogenated amorphous silicon was widely used in last decades in electronics. In recent years the nanocrystalline silicon are studying for many

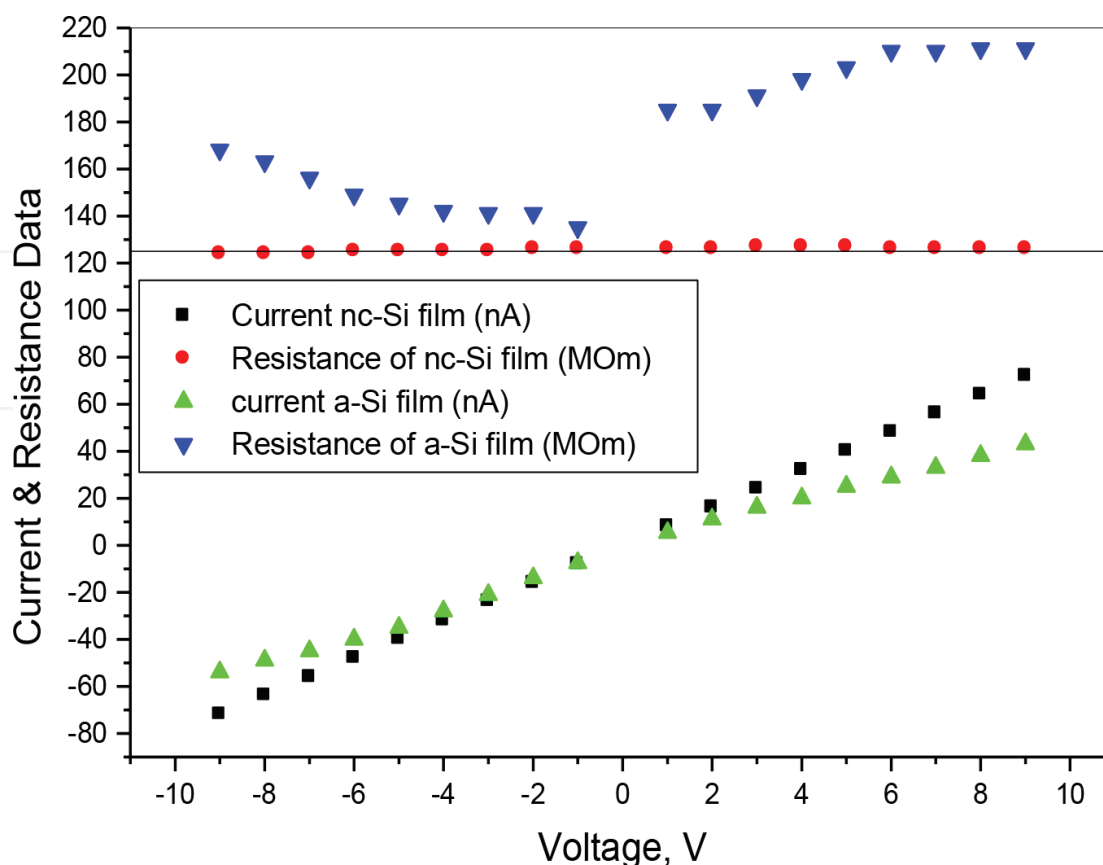


Figure 1. The current-voltage and ohm-voltage characteristics for two silicon films: amorphous and nanocrystallized.

technological applications. The structural transformation from crystal to disordered materials, however, is investigated very poor, mainly resulted in Staebler-Wronski photo-stimulated effect. However, the electric field applied to the nanostructured silicon thin film gives the new possibility to change structural order. Such kind of structural transformation is caused because of there are numerous defects inside the silicon film.

The anomalous characteristic of resistance-voltage can be explained by random distributed the point defects inside the amorphous film along with the hydrogen atoms, and existing the dipoles Si-O which turn to compensate the external electric field. But, for the nanocrystalline silicon film, the point defects are incorporated into silicon nanostructured net and cannot move freely, because there is a stable electric characteristic for nanocrystalline silicon film, and anomalous for amorphous.

The other new area of scientific interests is crystal-amorphous phase transformations by applying electric fields and role of local fields in phase transition from order to disorder. Because, it is important to investigate the point defects which can be responsible for local electrical fields generation in polarized media, such as dielectric silicon oxide media or semiconductor thin film of silicon. The main role plays here the silicon-oxide bonding in side thin film of silicon. Si-O dipoles play a dramatic role in crystal phase destruction by applying electric fields. The induced dipole moment by applied electric field can be written in the following form [12]:

$d_{i\alpha} = \alpha_0 \left(E_{i\alpha}^{(0)} - \sum_{j=1}^N \left(\delta_{\alpha\beta} - 3 \frac{(r_{ij})_\alpha (r_{ij})_\beta}{r_{ij}^2} \right) \frac{d_{j\beta}}{r_{ij}^3} \right)$; where $E_{i\alpha}^{(0)}$ is the field at the i -th monomer, r_{ij} is a relative vector between i -th and j -th monomer molecules, α_0 is the dipole polarizability. However, the Hamiltonian of semiconductor cluster can be surely expressed by using donor and acceptor states in bulk material [13]: $H = H_0 + H_D + H_A$, where H_0 is the Hamiltonian pure semiconductor for electron matrix elements of transitions between own conductive and valence bands, but H_D and H_A are the exchange energies matrix elements due to the donor and acceptor states, and for them it is clear be presented the following expressions:

$(H_D)_{ij} = \sum_k \frac{D_{ki}^2}{E - \varepsilon_k - \sigma_k} \delta_{ij}$; $(H_A)_{ij} = \sum_l \frac{A_{li}^2}{E - \varepsilon_l - \sigma_l} \delta_{ij}$; where D_{ki} and A_{li} are coupling between k -th donor state and l -th acceptor state, but the value $\sigma_{k,l} = \frac{1}{2} \left(\theta_{k,l} - i \sqrt{4\gamma_{k,l}^2 - \theta_{k,l}^2} \right)$ are the self-energy corrections which depend on locality of sites, and $\theta_{k,l} = E - \varepsilon_{k,l}$, and $\gamma_{k,l}$ are the ionization energy for electrons in sites, and overlap integral between atomic orbital for the donor in k -site and acceptor in l -site, respectively. Therefore, different explanations of polarization properties of semiconductor media can describe only partially in their own borders the electric induced local fields' appearance and various theoretical predictions based on them are not satisfied. The macroscopic description and molecular nanoscopic model are poor for investigating the mechanism of crystal semiconductor structures destruction by applied electric fields because the their dielectric functions is not so transparent for these complicated media, for example SiO_x , from one side, and their ratio between covalent and ion fractions of inter atomic bond are not so homogeneous, from the other side. Because, there is a necessity of detail investigation of nanoscopic nature of local fields appearance and mechanisms of crystal-amorphous phases' transformations.

The present work is devoted to the nature of local field appearance in silicon nanoscopic material and role point defects in phase transformation of material.

2. Experimental researches of field-assisted destruction of silicon nanocrystals

Nonlinear polarization associated with the phonons can be written as $P = \frac{1}{V} \sum_{i=1}^N \langle \mu \rangle_i = \frac{N}{V} \left(\frac{\partial \alpha}{\partial Q} \right)_0 \langle Q \rangle E$. Using these equations it is possible to obtain the wave equation for field: $\Delta E + \frac{\eta^2}{c^2} \frac{\partial^2 E}{\partial t^2} = -\mu_0 \frac{\partial^2 P}{\partial t^2}$, where $c^2 = \frac{1}{\mu_0 \varepsilon_0}$, $\eta = \sqrt{\frac{\varepsilon}{\varepsilon_0}}$.

Raman effect is result from the interaction of an electromagnetic field and optical phonon mode. The vibration wave $\langle Q \rangle = \frac{Q}{2} \exp(i(\omega_v t - k_v z)) + c.c$. The polarization at the Stokes frequency $P_S = \varepsilon_0 \chi_R(\omega_v) |E_i|^2 E_S$. Raman susceptibility

$$\chi_R(\omega_v) = \frac{N \left(\frac{\partial \alpha}{\partial Q} \right)_0^2}{4MV\epsilon_0} \frac{1}{\Omega^2 - \omega_v^2 - i(\Delta\omega_L)\omega_v}. \quad (2)$$

The microcrystal wave function is a superposition of Eigen functions with k vectors centered at k_0 . We suppose that $k_0 = 0$. If we are using the weighting function as Gaussian we will have

$$W(r, L) = \exp\left(-\frac{8\pi^2 r^2}{L^2}\right) |C(0, k)|^2 \cong \exp\left(-\frac{k^2 L^2}{16\pi^2}\right) \quad (3)$$

the normalized first-order correlation function $g^{(1)}(\tau) = \frac{\langle E^*(t)E(t+\tau) \rangle}{\langle E^*(t)E(t) \rangle}$. First-order coherence $g^{(1)}(\tau) = \exp(-i\omega(k)\tau - \frac{\Gamma_0}{2}\tau)$, where $\omega(k)$ is the phonon dispersion curve, Γ_0 is the natural line width. The spectrum of natural broadened value is $F(\omega) \propto \frac{1}{(\omega - \omega(k))^2 + (\frac{\Gamma_0}{2})^2}$. The phonon probability $\rho = \Psi_0 \Psi_0^* = u_0^2(r) \int d^3k |C(0, k)|^2$. The first-order Raman spectrum

$$I(\omega) \cong \int \frac{d^3k |C_0(k)|^2}{(\omega - \omega(k))^2 + (\Gamma_0/2)^2}. \quad (4)$$

For a microcrystalline and nanocrystalline silicon with sizes of crystals L if the weight function is Gaussian the first-order Raman spectrum is following [14]: $I(\omega) = \int_0^1 \frac{\exp(k^2 L^2 / 4a^2)}{[\omega - \omega(k)]^2 + (\Gamma_0/2)^2} d^3k$, $k = \frac{2\pi}{a}k$, a is lattice constant, k is dimensionless value, $\Gamma_0 \sim 3.6 \text{ cm}^{-1}$ line width of the Si LO phonons in c-Si. The dispersion of the LO phonon in c-Si $\omega^2(k) = A + B \cos(\pi k/2)$, where $A = 1.714 \times 10^5 \text{ cm}^{-2}$ and $B = 10^5 \text{ cm}^{-2}$ [15]:

$$I_{nc-Si}^{a-Si}(\omega) = 16\pi L(w, \rho) \int_{-\Delta q}^{\Delta q} \frac{|C(0, q)|^2 q^2}{4((\omega - \omega(q))^2 + \Gamma_T^2)} dq, \quad (5)$$

where local field factor can be written as

$$L(\omega, \rho) = \frac{\rho}{4\pi} \frac{(\epsilon_{c-Si}(\omega) - \epsilon_{SiO_x}(\omega))}{1 + (\epsilon_{c-Si}(\omega) - \epsilon_{SiO_x}(\omega))(\Lambda - \beta\rho)}$$

where q is a vector of inverted lattice, $2\pi/a$, a is a lattice constant. If the value λ_0 is the bond length Si-Si in bulk silicon, λ_1 is the weak bond resulted the silicon-oxygen surrounding. By the value of density of bonds is $N_{SiO} = 210^{21} \text{ cm}^{-3}$ and for crystalline silicon the density of silicon bonds $N_{Si-Si} = 510^{22} \text{ cm}^{-3}$ the lattice constants are following: $a_2 = 0.98 a_0$ and $a_1 = 0.996 a_0$.

For the silicon nanocrystalline and microcrystalline films the phonons can be generated in crystals by laser field or annealing. The wave of deformations can be generated by picoseconds

laser pulse [16]. The acousto-electric effect was observed in n-type germanium [17]. The electric field which was appeared by ultrasound waves can be estimated by using the formula $F = eE = \frac{q^2 S}{c^2 K T} \frac{\omega^2 \tau}{[1 + (\omega \tau)^2]}$, where E is an acousto-electric field, τ is a relaxation time $\tau^{-1} = (\frac{4}{3\tau_0}) + k^2 D$, D is a diffusion coefficient, The deformation potential causes the appearance of effective acoustical charge (**Figure 2**).

The nanocrystalline film was made by me using CVD method of silane diluted by hydrogen (gaze flow rates ratio is 1:10) at low temperature of substrate (80°C). The RF power was 20 W. Working pressure was 0.2 Torr. The crystalline volume fraction was 66%. The crystal orientations for nanocrystals were determined by means of X-ray diffraction technique (111) and their average size was 24 nm. The thickness of silicon film was more than 300 nm. **Figure 5** shows the changes in Raman scattering spectral data by applying the external electric field. It is seen, that there is phase destruction by the relatively high voltage. It is assumed that the nanocrystals which have grain boundary with oxygen atoms incorporated into silicon were destroyed in their crystal structure by Si-O dipoles reorientations caused by applied field. The initial crystal orientation was (111). The incorporated oxygen atoms are adsorbed in determined places. Their position results the appearance of numerous dangling bonds which are multiplied by the electric field and create the deep cracks in crystals. The crystal order is damaged along the axis that is perpendicular to (111). According to the Raman data for SiO₂ [18] the Raman spectrum of SiO₂ has the variation modes D1 (at 490 cm⁻¹) with defects and activation energies 0.14 eV and pure mode w_1 of Si-O-Si bridge. The sum dipole moment consists of dipole moment that is created due to the ellipsoidal shape and because of surface charges are appeared by silicon net deformation due to the oxygen incorporation in silicon SiO or hydrogen termination of dangling bonds and creation the SiH bonds: $P_{SiM} = \frac{8}{3} \pi a b^2 N_{SiM} \delta_{SiM} (b - a)$, where N_{SiM} , δ_{SiM} are the density of the bonds and partial charge for SiM bond (O or H), respectively (**Table 1**).

It is necessary to note that the fractal structure of several kinds of nanocrystals may cause the dramatically changes (four orders of magnitude) in intensity of Raman scattering due to existing of plasmon resonance into the gaps between the fractals [19]. The Raman intensity by these conditions can be expressed as

$$I = \frac{|\alpha|^2}{|E_0|^2} \int |\sigma(r)|^2 |E(r)|^4 dr. \quad (6)$$

where α is a polarizability and σ is a local conductivity of a fractal structure.

In addition, the light irradiation of amorphous silicon film causes the point defects generating and, mainly for amorphous hydrogenated silicon films, causes the appearance new dihydride configurations: (H-Si Si-H)₂(H-Si Si-H) and SiH₂ [20]. The two atoms of hydrogen in the SiH₂ unit show an average proton separation of 2.39 Å. Because, for the hydrogenated silicon nanocrystalline films under influence of applying the external electric field the hydrogen diffusion increases and polysilane chains are created, surely.

For poly-Si films with nanocrystals the values of densities of SiO and SiH bonds varies in wide range from 10¹⁹ to 10²¹ cm⁻³. The density of bonds were estimated for the poly-Si films

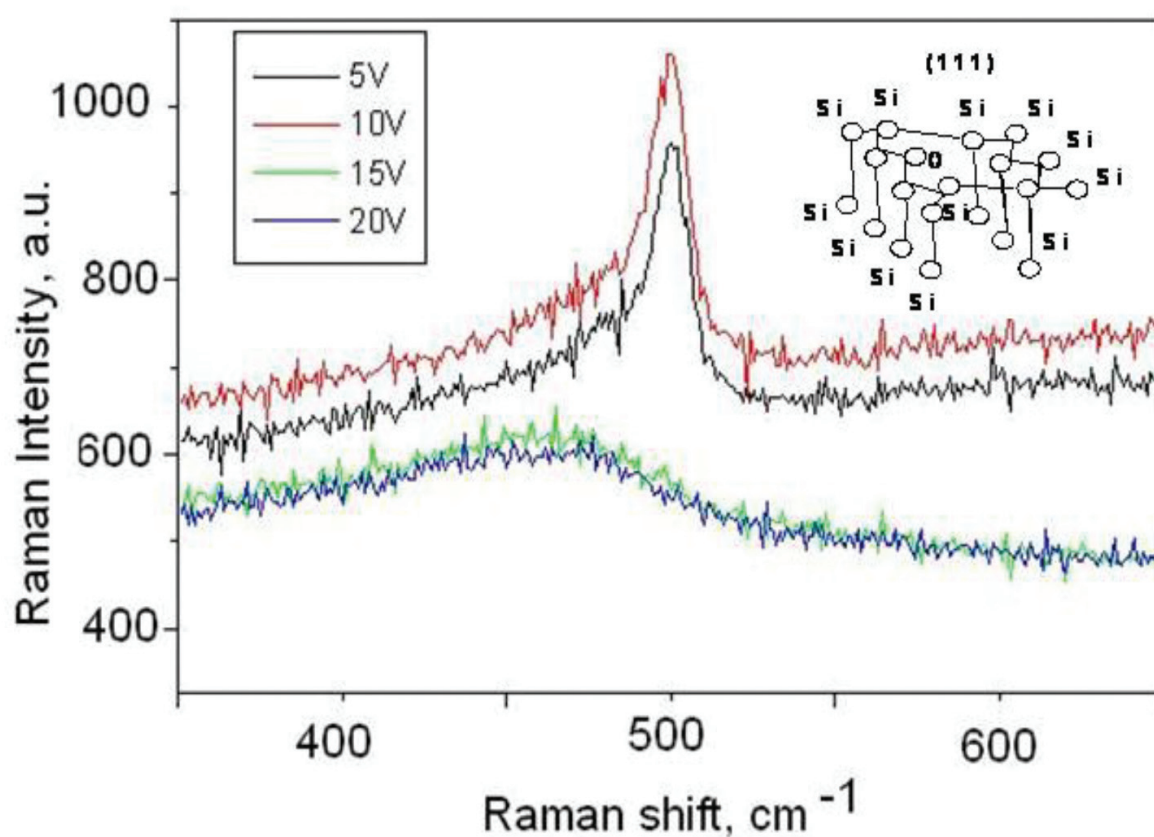
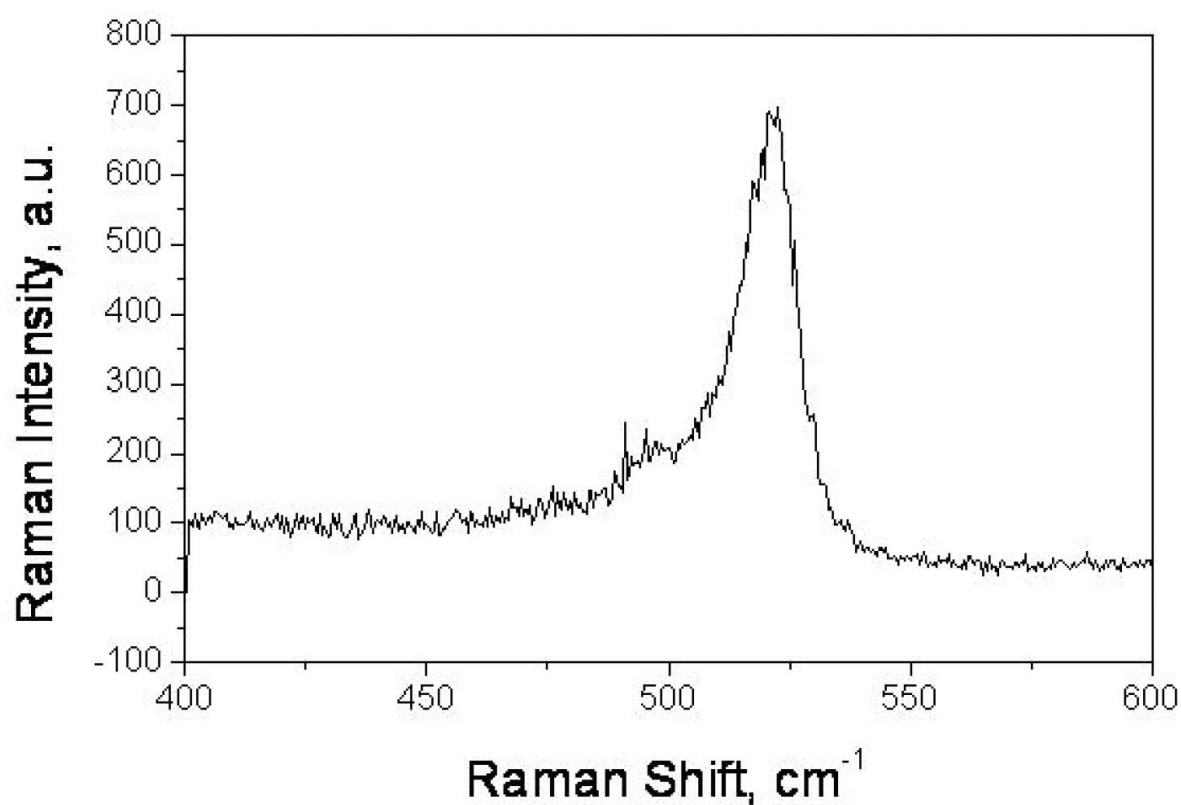


Figure 2. Raman spectra from nc-Si film with nanocrystal mean size 24 nm.

N_{DB}, cm^{-3}	$P_{\text{ellipsoid Debye}}$	$\Delta E = \mu E_{\text{ext}}, \mu\text{eV}$ by the $E_{\text{ext}} = 10^6 \text{ V/m}$	$\Delta E = \mu E_{\text{ext}}, \mu\text{eV}$ by the $E_{\text{ext}} = 10^7 \text{ V/m}$
10^{17}	1.1	20	200
10^{18}	10.8	200	2000

Table 1. The polarization of elliptic silicon grains evaluated by fixed N_{DB} and stark energy shifts for levels in electronic structure by external electromagnetic field.

prepared by using PECVD as following: for Si-Si bonding the density of bonds is equals to 510^{22} cm^{-3} , but densities of SiO and SiH bonds are 10^{21} cm^{-3} . In these films there is an oxygen contamination on the 2% level. The S/V ratio is 1.25%. I suppose that all the oxygen is concentrated around crystals in their grains boundaries. By these values of densities the dipole moments causes by surface charges can be estimated as $P_{\text{SiO}} = 0.04 \text{ D}$ and $P_{\text{SiH}} = 0.015 \text{ D}$. By applying external voltage it is clear that all Si-O dipoles move to compensate external field and destroy the crystal structure. Because, by applied electric field I observed the crystal phase destruction and SiO_x creation by using the Raman scattering data which correspond to the results reported in work [21].

3. Matrix Hamiltonian by small perturbation of Si-Si-Si bridge

For very small nanocrystals with sufficient ration S/V the mechanism of three elements simultaneous interaction is important for precise calculations. The energy shift due to the stress appearance for crystal orientation (111) is less than 0.14 eV for the vacancy-oxygen (VO) complex by a stress 0.3 GPa. The Hamiltonian of such system of n atoms as for example, -Si-Si-Si- and, particularly the Hamiltonian of interaction between atoms with indexes $k-1$ and $k+1$ can be explained in matrix form is given by using the operators of creation and elimination of boson particles, such as phonons: $H' = \alpha c_{k-1}^+ c_{k+1} + e.c.$ The Hamiltonian matrix of interaction between three atoms (with upper indexes $k-1$, k and $k+1$) in chain by a small perturbation α due to the VO appearance (for bonded Si_1 and Si_3 atoms without oxygen) can

be written as $\hat{H} = \begin{vmatrix} A_{11}^{k-1} & A_{12} & \alpha \\ A_{21} & A_{22}^k & A_{23} \\ \alpha & A_{32} & A_{33}^{k+1} \end{vmatrix}$. This matrix can be transformed into next triangular form:

$$\hat{H}' = \begin{vmatrix} A_{11} & A_{12} & \alpha \\ A_{21} & \hat{A}_{22} & \hat{A}_{23} \\ 0 & A_{32} & \hat{A}_{33}' \end{vmatrix}. \quad (7)$$

Here, the matrix elements $\hat{A}_{22} = A_{22} - A_{21}A_{11}^{-1}A_{12}$; $\hat{A}_{23} = A_{23} - \alpha A_{11}^{-1}A_{21}$; $\hat{A}_{33}' = A_{33} - \alpha A_{11}^{-1} \alpha - \hat{A}_{32}\hat{A}_{22}^{-1}\hat{A}_{23}$; $\hat{A}_{32} = A_{32} - \alpha A_{11}^{-1}A_{12}$; and according to the Vilandt-Hoffman theorem of matrix perturbation theory [22] the following inequalities can be written.

$\left(\sum_{i=1}^n |(\lambda_{Ai} - \lambda_{Ai})|^2\right)^{1/2} \leq \|(A + E) - A\|_E$ or $\hat{\lambda}_{33}^2 \leq \lambda_{33}^2 + \frac{a^2}{\lambda_{11}}$. Because, for the creation operator $\hat{c}_{2k+1}(t)$ is true the following expression $\hat{c}_{2k+1}(t) = c_{2k+1}(t)\exp\left(-i \int_0^t \frac{a^2}{E \lambda_{11}} d\tau\right)$. Therefore, the dispersion curve is written as $\omega_{phonon} = \omega_0 \pm \xi$, where ω_0 dispersion curve without applied field (for energy 0.14 eV the estimated additional frequency is less than 3.4×10^{13} Hz, and additional frequency $\xi = \frac{a^2}{\lambda_{11}}$ by stress due to the appearance of VO defects. According to the proposed model that is suitable for description Raman scattering phenomena caused by nano-sized cavities it is assumed that the results Raman frequency of radiation after scattering can be written as $\omega_s = \frac{\mu E}{\hbar}$; where $\mu = dQ$ is dipole moment of nanocrystal, E is field, d is the size of crystal, Q is charge (Figure 3).

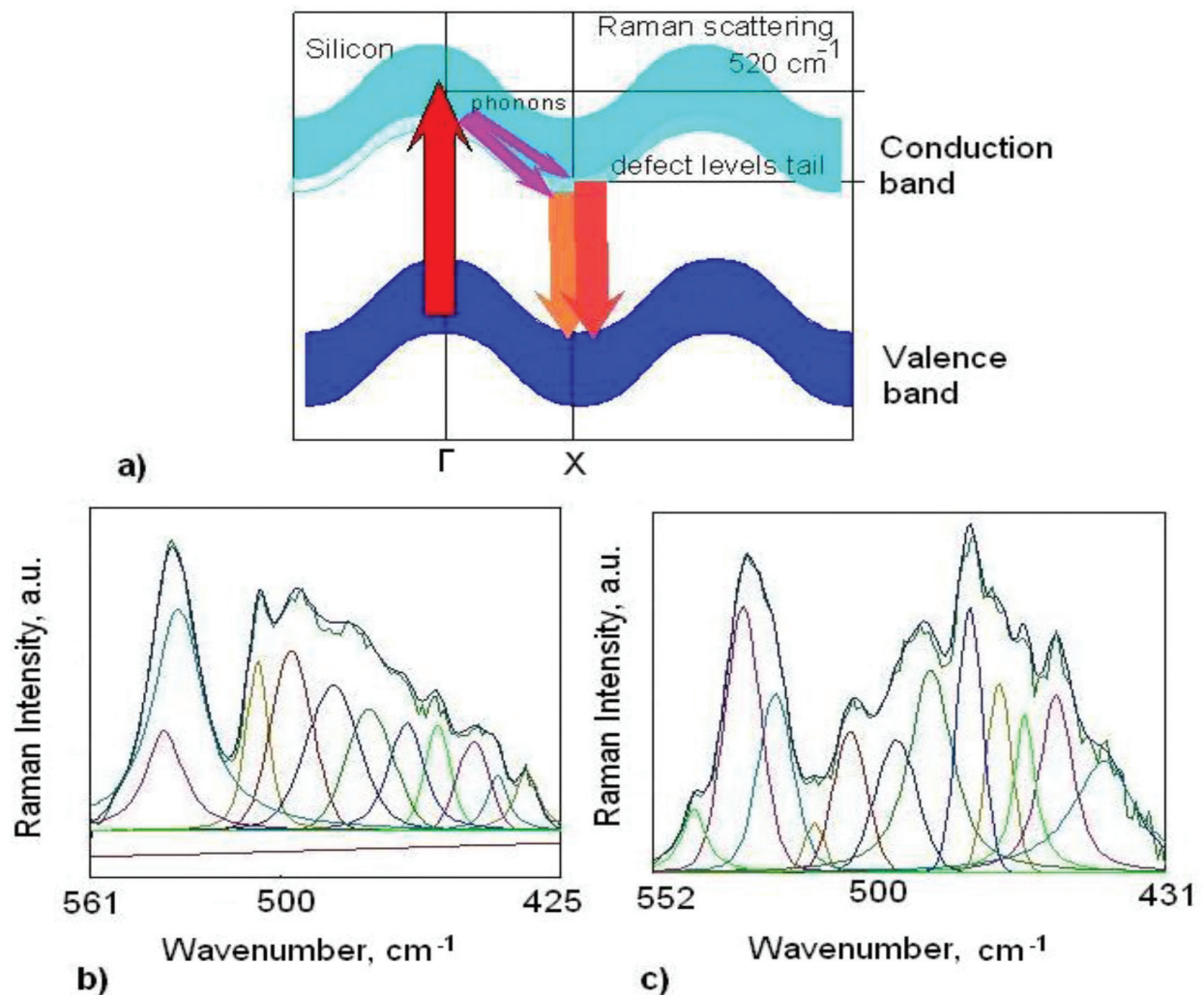


Figure 3. Scheme of Raman scattering of photons on phonons (a) and Raman spectra for silicon film without external field (b) and by applied external electric field with additional spectral peak at 540 cm^{-1} which was created due to the defects generating by electric field (c).

4. Model of polaron state in silicon nanocrystals

The probability of changing the polarization state from one to another can be described by using Golden rule of Fermi

$$W_{ij} = \frac{2\pi}{\hbar} \sum_k \left| \langle \psi_i | H | \psi_j \rangle \right|^2 \delta(E_j - E_i - \hbar\omega_{polar}), \quad (8)$$

where $\omega_{polar} = \frac{pE}{\hbar}$ is a polarization energy that can be expressed in frequency units. Matrix element for such changing of polarization state from i to state j , according to theoretical work of V. Lakhno [23], can be written as

$$\langle \psi_i | H | \psi_j \rangle = \hbar k \sqrt{\frac{\hbar N_1}{6V\omega_{polar}\epsilon m}} \left| \int \Psi_{ic} \frac{e^{ikr}}{\sqrt{V}} d^3r \right|^2, \quad (9)$$

where V is a nanocrystal volume (**Figure 4**).

The second-harmonic generation is forbidden for center symmetric crystal such as bulk silicon because the sum dipole moment is zero, but is possible due to the surface breaking symmetry and quadruple terms contributions. The opposite situation is for nanostructured oxidized silicon film, the surface area for a great amount of nanocrystals is significant, the breaking symmetry is permanent and lateral isotropic. The oxygen atoms with concentration up to the values of 10^{20} – 10^{21} cm^{-3} show the sharp increase in SHG by increase in polarization properties of material, that have its properties as silicon nanocrystals, as silicon oxide inclusions. **Figures 5 and 6** illustrate the SHG spectra of radiation reflected from silicon films.

The reflected SHG response was measured by using the radiation of optical parametric oscillator/amplifier pumped by the third harmonic (355 nm) of a Q-switched Nd: YAG laser (Spectra-Physics, MOPO 730) at a 10 Hz repetition rate with spectral range between 440 and 1700 nm. The bandwidth of radiation is 0.3 cm^{-1} . The SHG response was detected by a photomultiplier tube

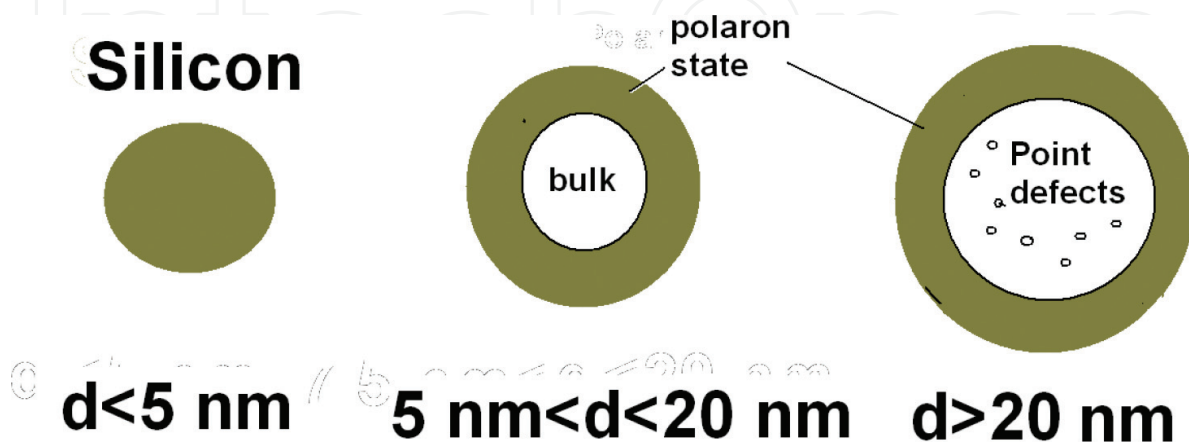


Figure 4. Silicon nanocrystals with different sizes by applying external electric field have various electronic structure: with polaron state in all volume of nanocrystal, and partially polarized nanocrystal according to relation between the values of size and "skin"-layer or depth of field penetration.

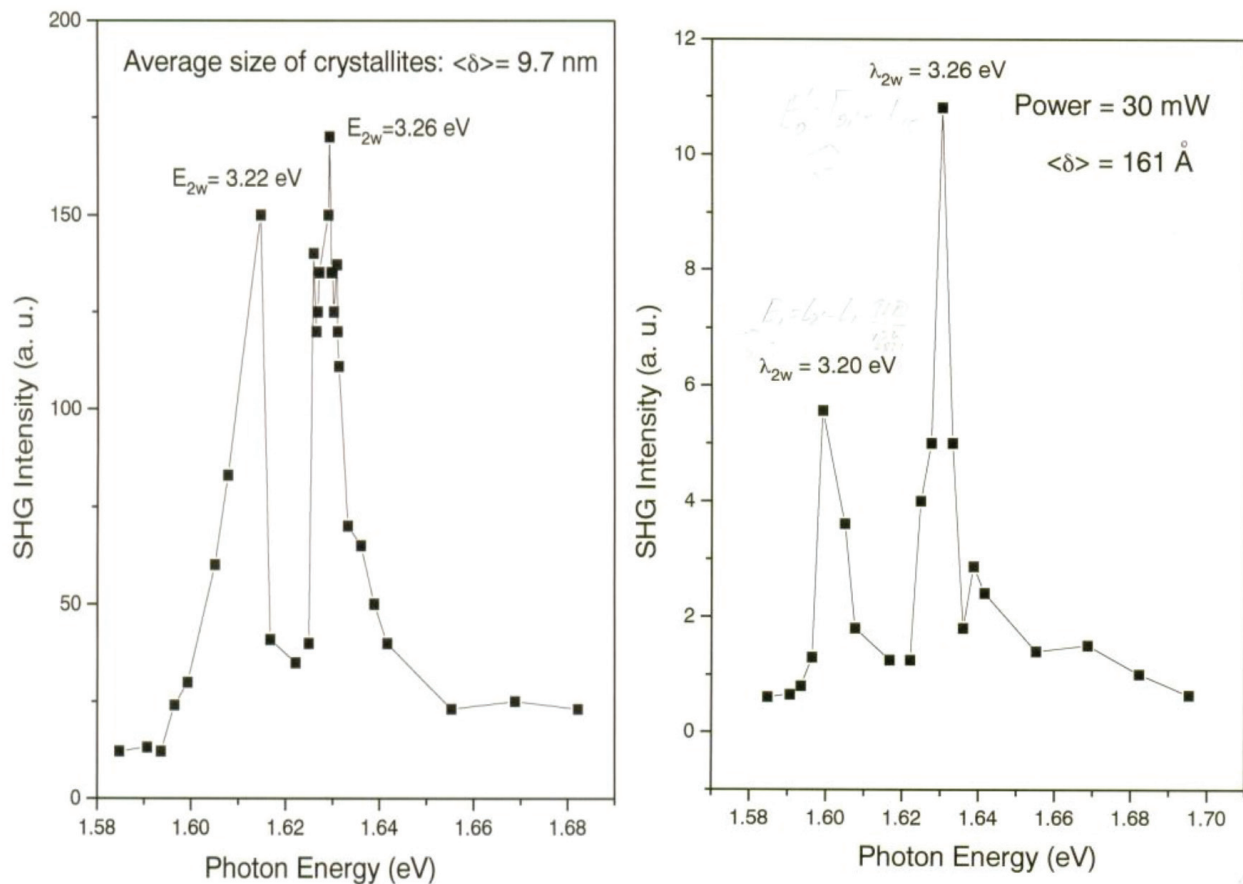


Figure 5. SHG spectra for $\chi_{xxx}^{(2)}$ component of susceptibility.

and gated electronics with an average of 100 pulses. The linear polarized radiation was focused on the surface of the sample at the angle 45° and detected SHG signal was observed at the angle 45° , too. Such optical scheme arrangement was useful for surface contributors' detection from the silicon surface (111). The diameter of irradiated spot was 0.5 mm. The energy of the primary laser beam was 4 mJ. The second-harmonic intensity can be written as

$$I(2\omega) = \frac{32\pi^3\omega^2\sec^2\theta_{2w}}{c^3\varepsilon(\omega)\varepsilon^{1/2}(2\omega)} |L(2\omega, \rho_{\min})L^2(\omega, \rho_{\min})|^2 |\chi_2(\omega)|^2 I^2(\omega) \quad (10)$$

where the $L(\omega, \rho)$ value is a local field factor of film with crystalline volume fraction equals to $\rho = 70\%$.

The SHG intensity as a function of the average grain size in poly-Si films, with crystalline volume fraction 70%, is presented in **Figures 5 and 6** where

$$K = \frac{I_{\exp}}{I_{\exp}^{\min}} \frac{|L(2\omega, \rho_{\min})L^2(\omega, \rho_{\min})|}{|L(2\omega, \rho)L^2(\omega, \rho)|} \quad (11)$$

is normalized SHG signal, $L(2\omega, \rho)$ and $L(\omega, \rho)$ are the factors of the local field, where ε_c and ε_a are dielectric functions of crystalline and amorphous silicon, respectively. For sphere depolarization factor Λ is equal to $1/3$, β is the Lorentz constant (for homogeneous spherical

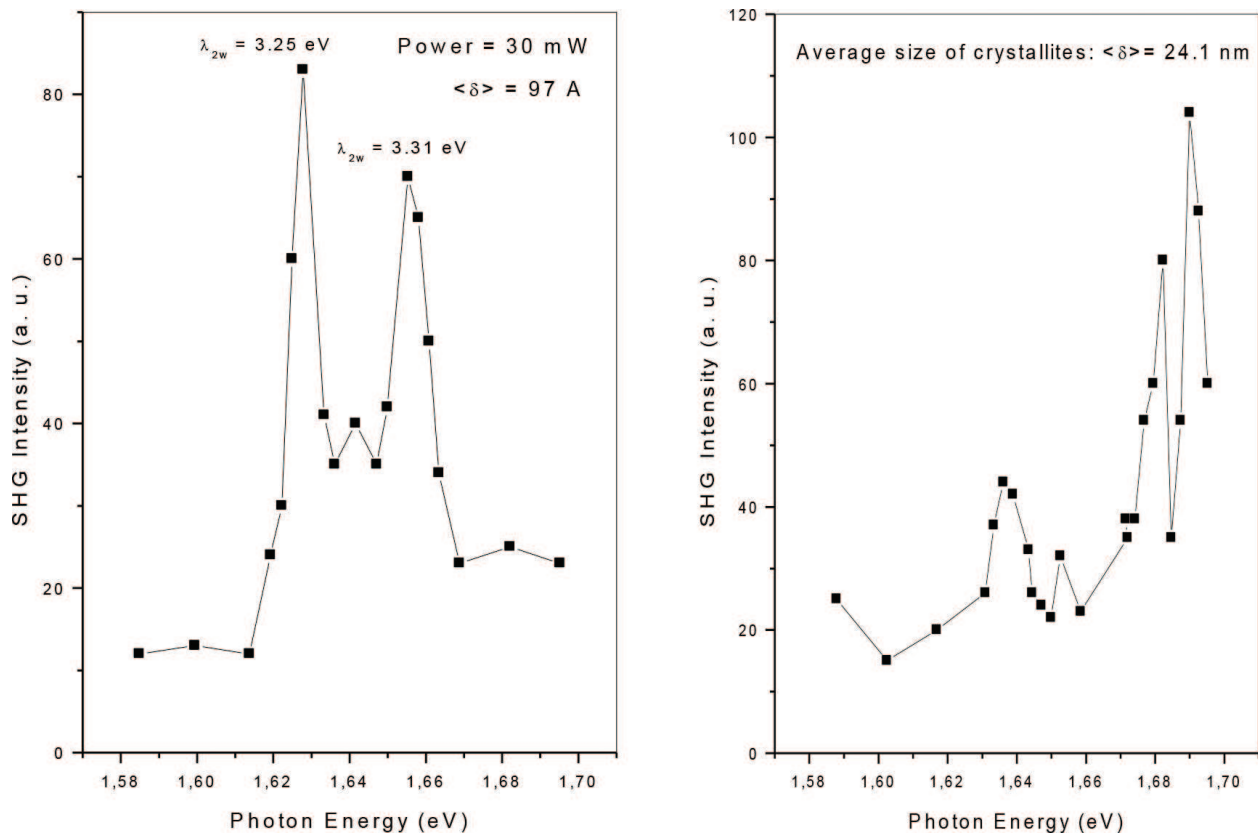


Figure 6. SHG spectra for $P_{in} \rightarrow P_{out}$ laser scheme and $\chi^{(2)}_{xxx}$ component of susceptibility.

surrounding $\beta = 1/3$). For calculations the following estimated values were $\lambda_w = 1064$ nm, $\lambda_{2w} = 532$ nm, $\epsilon_c'(\omega) = 13$, $\epsilon_c''(\omega) = 0.03$, $\epsilon_a'(\omega) = 12$, $\epsilon_a''(\omega) = 0.23$, $\epsilon_c'(2\omega) = 18$, $\epsilon_c''(2\omega) = 0.5$, $\epsilon_a'(2\omega) = 18$, $\epsilon_a''(2\omega) = 7.5$. Resonance spectra consist of two sharp peaks. The peak at 1.6 eV is caused by SHG response due to $E_0' = \Gamma_{21} - \Gamma_{15}$ transition. We suppose that the second peak can be recognized as SHG response due to $E_1 = L_{2'} - L_1$ transition in silicon nanocrystallites.

$$L(\omega, \rho) = \frac{\rho}{4\pi} \frac{(\epsilon_c(\omega) - \epsilon_a(\omega))}{1 + (\epsilon_c(\omega) - \epsilon_a(\omega))(\Lambda - \beta\rho)}$$

The contribution of point defects as deviations of local fields and external applied electric field for a phonon generation in silicon nanocrystalline can be described by using the perturbation theory. The model Hamiltonian's matrix for two-level system including the point defect as small perturbation ε that causes the violence of phonon energies of system E_1 (for unperturbed state) and E_2 (perturbed state):

$$\begin{pmatrix} E_1 & \varepsilon \\ \varepsilon & E_2 \end{pmatrix} \quad (12)$$

The changes in Eigen values from the E_1 and E_2 by the field $E = 0$ to the new values of energies are following

$$\lambda_{1,2} = \frac{E_1 + E_2}{2} \pm \sqrt{\frac{1}{4}(E_1 - E_2)^2 - E_1 E_2 + \varepsilon^2}. \quad (13)$$

It is assumed, that the field value ε determined as linear combinations of external applied field and all local deviations due to film structural disorder. We assume that there is no strict disorder media, but some small disorder is determined. $\varepsilon \approx (E_1 - E_2)$; $\Delta E \approx 2(E_1 - E_2) = 2\Delta$. Therefore, by a small perturbation of system $\varepsilon \leq (E_1 - E_2)$, the energetic gap between the two levels which are located closed each to other increases from the zero value to 2Δ . The value of perturbation of atomic orbital for dimer molecular like assembly Si-Si in a point defect as $(VO)^{-}$ can be evaluated by using the energy of their interaction of atoms with dipole Si-O, that has its polarized charge $0.2 e$: $F = \frac{1}{4\pi\epsilon_0} \frac{0.2e^2}{r^2}$; where r is a distance from the dimer Si-Si to dipole Si-O equals to $1-2 \text{ \AA}$.

From the other side, for drift of particle, such as hydrogen atom, by driving forces in condensed matter can be expressed by using formula for force $F = \frac{H_M}{kT} k \nabla T$, where H_M is an enthalpy or energy of transport by heat, ∇T is a gradient of temperature [24]. For elastic medium the force that treats the defect is given by using stress value σ and displacement field of defect in its surrounding medium as u : $F = \int_{\Sigma} (u \nabla \sigma - \sigma \nabla u) ds$. David Emin studied the deformable lattice in 1972 [25] by using short-range electron-lattice interaction in dielectric or semiconductor materials which have weakly coupled electron-lattice interactions or small polaron states, the distortion related energy of which expressed in terms of distortion parameter x , $E = \frac{1}{2} M \omega^2 x^2$, the energy reduction due to the linear electron-lattice interaction as $E = Ax$.

5. Modular group translation model for crystal phase destruction by applied electric field

I propose the modular group translation (MGT) model for crystal phase destruction by applied electric field for explanation the Raman data which are on **Figure 7** and show the dramatic

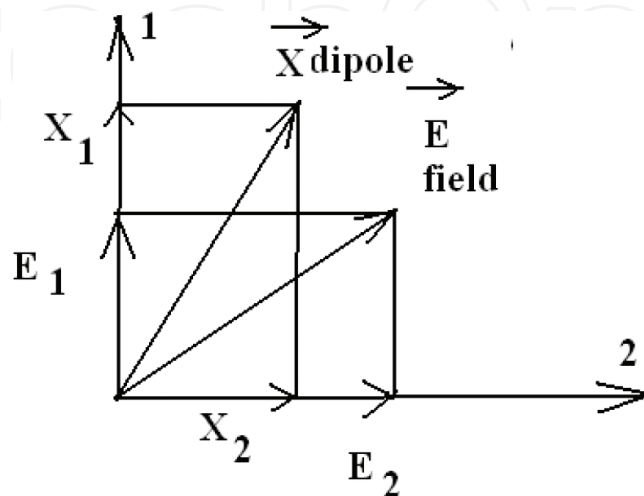


Figure 7. Scheme of dipole's and electric field vectors location on 2D plate.

changes in silicon crystal phase related spectral component at 520 cm^{-1} due to the applying electric field.

It is assumed that the electric fields of external field and local polarized field can be written as $\vec{E}_1 = \begin{pmatrix} E_{11} \\ E_{12} \end{pmatrix}$; $\vec{E}_2 = \begin{pmatrix} E_{21} \\ E_{22} \end{pmatrix}$; $\vec{X}_1 = \begin{pmatrix} X_{11} \\ X_{12} \end{pmatrix}$; $\vec{X}_2 = \begin{pmatrix} X_{21} \\ X_{22} \end{pmatrix}$; for applied and local electric fields, and for dipoles vectors on 2D plate. For free energy it is easy to write the expression by using binding energy and energies of dipoles in external field and local field: $F = \frac{1}{2} \sum_N N_i (E_j - \delta Q_j \vec{E}_j \cdot \vec{x}_j)$, where N_j is a number of neighbor atoms, \vec{E}_j and \vec{x}_j are the vectors of electric field and dipoles along the j direction. For j components of free energy along the axis 1 and 2 on 2D plate it is surely can be presented other form of such formula:

$$F_1 = E_1 - \delta Q_1 E_{11} x_{11} - \delta Q_2 E_{21} x_{21}$$

$$F_2 = E_2 - \delta Q_1 E_{12} x_{12} - \delta Q_2 E_{22} x_{22}.$$

For analysis of deformation by applying the external electrical field it is clear to use ratio between free energy components for different bonding and directions:

$\frac{F_1}{F_2} = \frac{E_1 - \delta Q_1 E_{11} x_{11} - \delta Q_2 E_{21} x_{21}}{E_2 - \delta Q_1 E_{12} x_{12} - \delta Q_2 E_{22} x_{22}}$; and, according to the conservation law for a system shown on **Figures 8, and 9** charge neutrality for all elements of system influenced by electric field equals to nonzero, it can be possible to write the following formula:

$$\delta Q_1 E_{11} x_{11} + \delta Q_2 E_{21} x_{21} + \delta Q_1 E_{12} x_{12} + \delta Q_2 E_{22} x_{22} = 0.$$

Accordingly, the ratio between the polarization charges for two dipoles inside the electric field is given by

$$\frac{\delta Q_1}{\delta Q_2} = \frac{E_{11} x_{11} + E_{12} x_{12}}{E_{22} x_{22} + E_{21} x_{21}}; \text{ or } \delta Q_2 = -\delta Q_1 \frac{E_{22} x_{22} + E_{21} x_{21}}{E_{11} x_{11} + E_{12} x_{12}} = -A \delta Q_1.$$

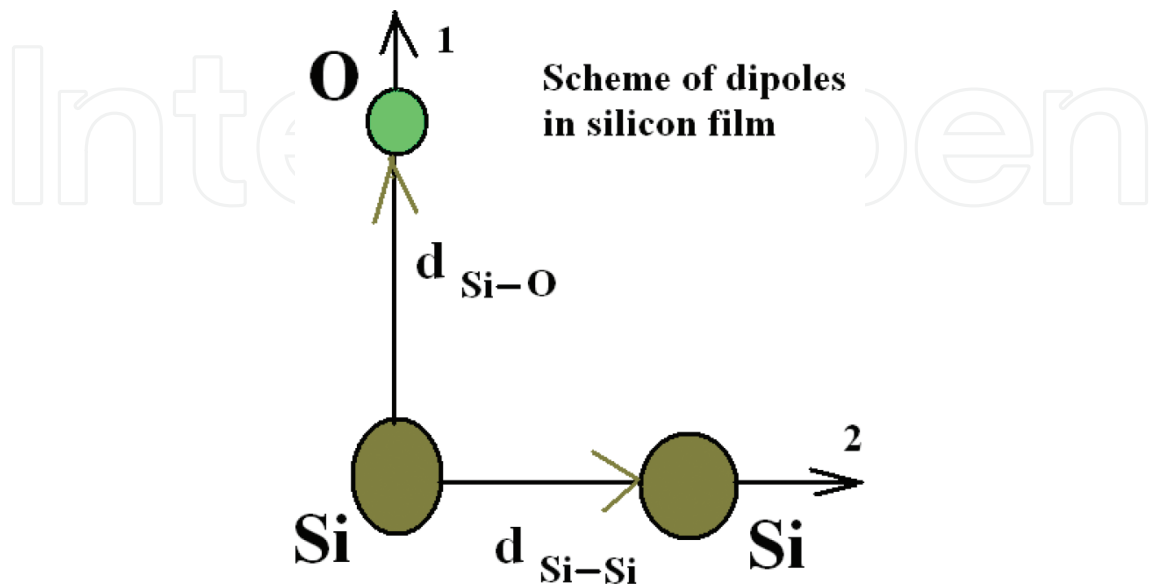


Figure 8. Scheme of arrangement of dipole vectors along the axis.

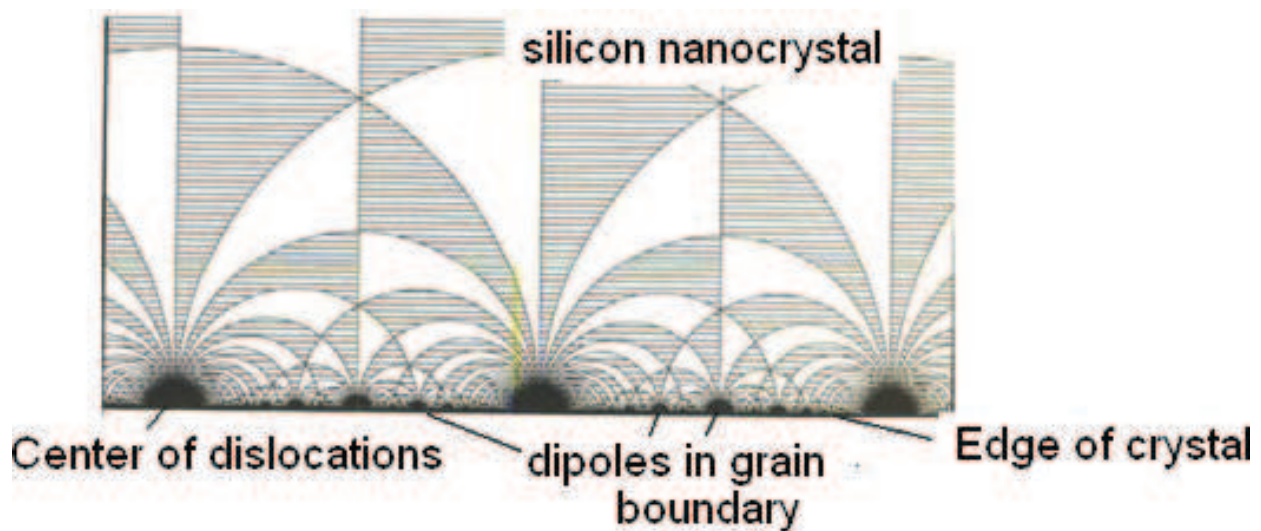


Figure 9. Scheme of nanocrystal's destruction by external electric field.

The first dipole is devoted to the description of electrical polarization properties of Si-Si bond, but the second – Si-O bond. By substituting the expression for Si-O polarization charge in expression for free energy we can easily to obtain the following expression

$$F_1 = E_1 - \delta Q_1(E_{11}x_{11} - AE_{21}x_{21})$$

$$F_2 = E_2 - \delta Q_1(E_{12}x_{12} - AE_{22}x_{22}).$$

The relation between the deformation values along the 1 and 2 axis can be used for analysis the translations consequences of modular group.

$\frac{W_1}{W_2} = \frac{(E_{11}x_{11} - AE_{21}x_{21})}{(E_{12}x_{12} - AE_{22}x_{22})}$; or $\frac{W_1}{W_2} = \frac{(p+r)}{(q+s)}$; where the first pair p, q describe the translation result applied field, but the second pair r, s causes the translation due to the local and external fields interaction with Si-Si dipoles. Crystal phase destruction can be generated by using significant values of electric field combining with sufficient density of Si-O dipoles inside the silicon film (**Figure 10**).

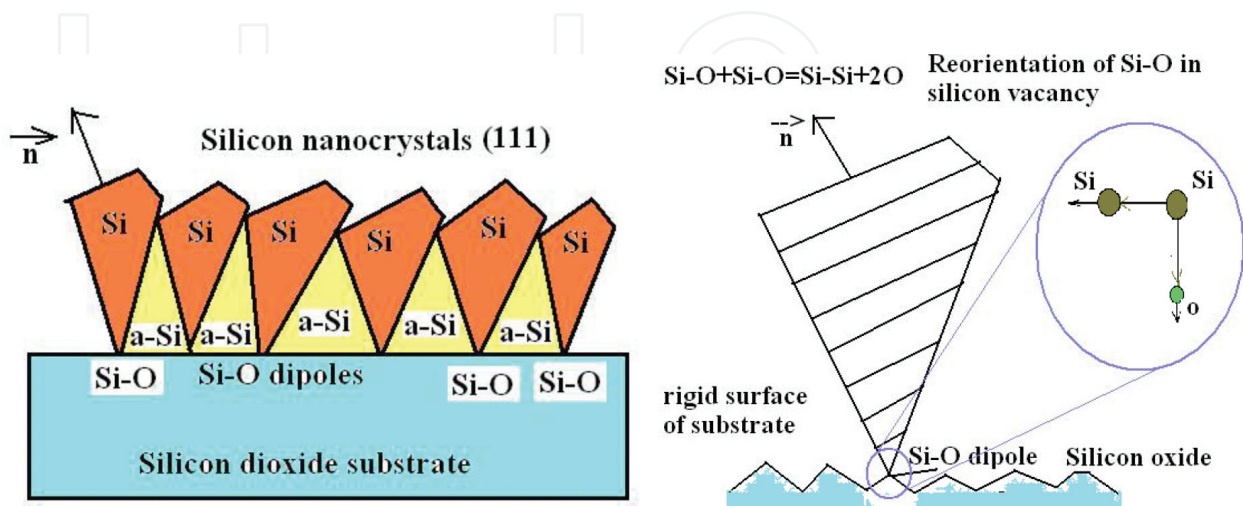


Figure 10. Scheme of silicon nanocrystal film with orientation (111) and precipitate of crystal growth on silicon dioxide substrate with nuclear silicon-oxide dipole in the top of pyramid.

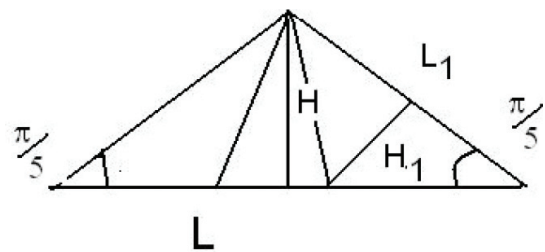


Figure 11. Scheme of geometrical transformation the primary triangle with L and H parameters into triangle 1 with parameters L_1 and H_1 .

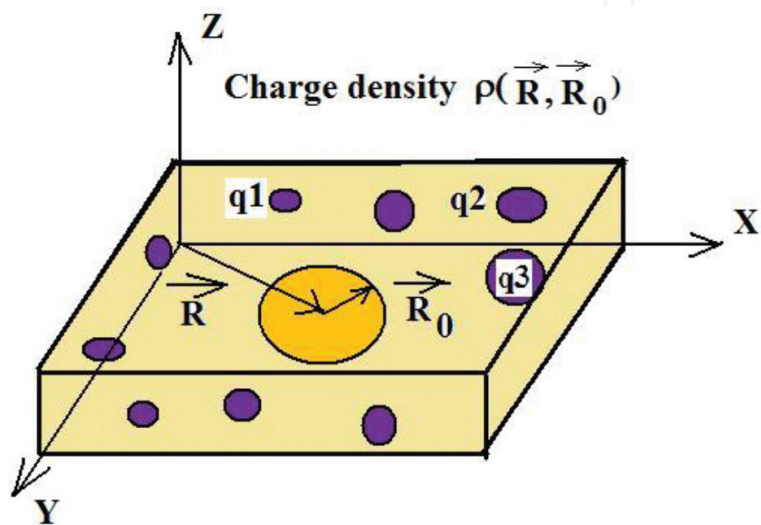


Figure 12. Scheme of charges density for anisotropic and non-homogeneous media.

Transformations which create the low dimensional model structure are illustrated on **Figures 11** and **12** and are explained as combination of modular group transformation of two-dimensional nanocrystal and Knop triangular transformations into Kantor dust set or fractal structure with low dimension. The surface and interface point defects and impurities cause the local electric fields which can generate by applying external field great values of field.

6. Possible scenario of nanocrystal destruction: from bulk silicon to Kantor dust

Model of phase destruction by modular group substitution [26] which consists of arc series and Knop transformation of two-dimension area under arc through the triangular decomposition [27] to one dimensional structure. The down picture illustrates the creation of Kantor dust by dividing the triangular angle on the top and neglecting the area of triangle in the middle of primary triangle area. Such nonlinear triangular transformations can be caused by a point defects and impurities which were included in bulk silicon net of nanocrystal.

$$\begin{aligned}
 S &= \frac{1}{2}HL., \\
 S_1 &= \frac{1}{4}L_1^2 \operatorname{tg}(\pi/5). \\
 H &= \frac{1}{2}L_1 \operatorname{tg}(\pi/5), \\
 L_1 &= \sqrt{H^2 + \frac{L^2}{4}}; L = \frac{2S}{H}; H^2 = S \operatorname{tg}(\pi/5); \\
 S_1 &= \frac{1}{4} \left(H^2 + \frac{S^2}{H^2} \right) \operatorname{tg}(\pi/5); \frac{S}{S_1} = 4 \frac{1}{(\operatorname{tg}^2(\pi/5) + 1)} = 2.63
 \end{aligned}$$

For such transformation the equations for triangular quantities $X_N = 2X_{N+1}$ and for areas $S_{N+1} = 0.38 \cdot S_N$. The estimated value of Hausdorff dimension for such mathematical set is $d = \frac{\ln 2}{\ln 2.63} = 0.72$.

7. Classical and quantum mechanical models of charge and current densities

We have to propose the new model that is more suitable to explain electric properties of nanometrical scale media with strong anisotropic and non-homogeneous properties (see **Figure 12**). It will be necessary to describe the further possibility to design new nanoelectronic devices based on quantum conductivity properties and atomic scale sizes.

$$\begin{aligned}
 Q(R) &= 4\pi \int \rho(R, R_0) R_0^2 dR_0; \\
 V &= \frac{4}{3} \pi R_0^3; \\
 dV &= 4\pi R_0^2 dR_0.
 \end{aligned} \tag{14}$$

For current density of homogeneous media with charge density ρ in classical theory we usually use the formula

$$\begin{aligned}
 \vec{j} &= \frac{\vec{I}}{S} = \frac{N \vec{v} Q}{S} = \frac{\vec{v} \rho}{S}; \\
 \rho &= NQ
 \end{aligned} \tag{15}$$

For ρ value of non-homogeneous anisotropic media it is possible to use the expression:

$$\begin{pmatrix} \rho_{XX} & \rho_{XY} & \rho_{XZ} \\ \rho_{YX} & \rho_{YY} & \rho_{YZ} \\ \rho_{ZX} & \rho_{ZY} & \rho_{ZZ} \end{pmatrix}. \text{ For current density the following form is given:}$$

$$\vec{J} = \frac{e}{S} \begin{pmatrix} \rho_{XX} & \rho_{XY} & \rho_{XZ} \\ \rho_{YX} & \rho_{YY} & \rho_{YZ} \\ \rho_{ZX} & \rho_{ZY} & \rho_{ZZ} \end{pmatrix} \begin{pmatrix} v_X \\ v_Y \\ v_Z \end{pmatrix}; \text{ where the absolute value of vector } |\vec{e}| = 1. \text{ To determine the}$$

charge density and current density on nanoscopic scale the quantum mechanical approach is applicable by the way

$$\rho = e\Psi^*\Psi; \quad J_{ij} = \frac{i\hbar e}{2m} \left(\Psi_{3piSi} \frac{\partial \Psi_{3pjSi}^*}{\partial r_j} - \Psi_{3pjSi}^* \frac{\partial \Psi_{3piSi}}{\partial r_i} \right).$$

It is clear, that such approach is approximate and can be applicable to study the electric properties of point defects.

Nonlinear polarization concludes as linear as nonlinear terms: $P = \alpha E$, where α is a linear polarizability. Canonical equation for electro-magnetic fields can be written by using the Maxwell equations by a simplification of model and assuming that the first order of derivatives are much more than others. The second supposal is that the solution can be explained as harmonic function. It is clear, that the equation for the field for second harmonic can be presented in the following form

$$\frac{\partial E}{\partial z} = -\frac{\sigma}{2} \sqrt{\frac{\mu}{\epsilon}} E \quad (16)$$

It is supposed that currents which was created due to the electromagnetic field of second harmonic generation and induced in nanocrystals dominate in surface layers and grain boundaries. Because, such currents can be explained by the first term in equation and relate to absorption and emission of photons. Equation (17) can be written in suitable form:

$$\frac{\partial E}{\partial z} = -\frac{J}{2} \sqrt{\frac{\mu}{\epsilon}} \quad (17)$$

Because, the surface current can play a significant role in nanostructured silicon film and the current density can be written as following J:

$$J = \sigma E = -\frac{2}{\sqrt{\mu}} \frac{\partial E}{\partial z} \sqrt{\epsilon}; \quad E(z) = E(0) \exp\left(-\frac{\sigma \sqrt{\mu}}{2\sqrt{\epsilon}} z\right). \quad (18)$$

By a symmetrical form of wave functions $\Psi \approx \exp(i(kx - \omega t))$ the current value is zero. By a bonding of p orbital of silicon atoms for bonding and antibonding cases the energy gap between them is estimated as 10 μeV and their energetic location is closed to a bottom of conductivity band $E_c - 0.17 \text{ eV}$.

$$\Psi(t) = \left(a\Psi_{3piSiA} \exp\left(\frac{-iE_A}{\hbar} t\right) + b\Psi_{3pjSiB} \exp\left(\frac{-iE_B}{\hbar} t\right) \right); \Delta E = E_B - E_A = 10 \mu\text{eV}. \quad (19)$$

For two energetic levels (A and B) which are situated closed to each other the expression for the current density is following:

$$J_{ij} = \frac{i\hbar e}{2m} \left[a^2 \left(\Psi_{3piSiA} \frac{\partial \Psi_{3pjSiA}^*}{\partial r_j} - \Psi_{3pjSiA}^* \frac{\partial \Psi_{3piSiA}}{\partial r_i} \right) + b^2 \left(\Psi_{3piSiB} \frac{\partial \Psi_{3pjSiB}^*}{\partial r_j} - \Psi_{3pjSiB}^* \frac{\partial \Psi_{3piSiB}}{\partial r_i} \right) + \right. \\ \left. + ab \left(\Psi_{3piSiB} \frac{\partial \Psi_{3pjSiA}^*}{\partial r_j} - \Psi_{3pjSiA}^* \frac{\partial \Psi_{3piSiB}}{\partial r_i} \right) \exp \left(\frac{-(E_B - E_A)}{\hbar} t \right) + \right. \\ \left. + ab \left(\Psi_{3piSiA} \frac{\partial \Psi_{3pjSiB}^*}{\partial r_j} - \Psi_{3pjSiB}^* \frac{\partial \Psi_{3piSiA}}{\partial r_i} \right) \exp \left(\frac{(E_B - E_A)}{\hbar} t \right) \right].$$

The values of currents for two energy states A and B are different due to the difference in their energies, and their occupations are also varied because they depends on Boltzmann distribution for unperturbed case, and for the laser excitation of carriers they distributed according to the Gauss distribution. Because, the current of charges depends strictly on energetic location of defects levels which are closed to the bottom of conductivity band of silicon. Therefore, the nonzero current is appeared because the field of SHG is applied in silicon nanocrystals. The current spectrum has a resonant energetic peak by the electron energy became equal to the energy of defect level:

$$J \approx \frac{2\hbar e}{m} ab \cos \left(\frac{\Delta E}{\hbar} t \right). \quad (20)$$

The dipoles-field interaction causes the appearance of oscillations on frequencies $\Omega_1 = \frac{\mu_1 E}{\hbar}$ and $\Omega_2 = \frac{\mu_2 E}{\hbar}$, which by reemission result in radiation with various harmonics such as $2\omega \pm \Omega_1$, $2\omega \pm \Omega_2$, $2\omega \pm \Omega_1 \pm \Omega_2$. The estimates for the values a and b as a levels' widths are following $a = \frac{\Delta E_a}{\Delta E_a + \Delta E_a} g_a$; $b = \frac{\Delta E_b}{\Delta E_a + \Delta E_a} g_b$, and by using the Erginsoy formula for semiconductors impurities it is possible to determine the sizes of local area for such kind of effect $\sim R^3$, where R is a size of area of surface SHG assisted currents are generated. Therefore, there is a surface current in nanocrystals which are generated by applying the SHG fields. Such currents are caused by repolarization of pairs of atoms of silicon by their distribution of the surfaces of all nanocrystals irradiated by laser light. By this irradiation the times of repolarization are much more than period of oscillation of electromagnetic field of laser radiation, because there is absorption of radiation.

The free energy for nanocrystal with volume V can be expressed as following: $F = F_0 - \frac{\kappa V E^2}{2}$. By using determination of deformation of solid, it is possible to use the other definition for free energy by using the Lamé coefficients η and ν [28]: $F = F_0 + \frac{\eta}{2} u_{il}^2 + \nu u_{ik}^2$, By equating of two right parts from expression ((11)) and (12), it is easy to obtain the result: $-\frac{\kappa V E^2}{2} = \frac{\eta}{2} u_{il}^2 + \nu u_{ik}^2$.

The estimated value of free energy to destroy the silicon crystal phase is following $F < 1.23 \cdot 10^{-4} \text{ J/cm}^2$. There are various preliminary states between stabile Si-Si bonds and broken bonds. The bond length distortion is varied from 0–15% of initial bond length. There are minima in potential energy for hydrogen which are varied from 1.3 eV to 2.3 eV. The Coulomb force driving the migration of charged impurity or defect can be written as $F = ZeE$; where the value of Z is an effective charge of defect, E is applied electric field. According to [28] the force due to the appeared interstitial atom is written as an Eshelby formula $F = \alpha \frac{4}{3} \pi r_0^3 \nabla \text{Tr}(\sigma)$, where $\text{Tr}(\sigma) = \sigma_{11} + \sigma_{22} + \sigma_{33}$, σ is a stress, r_0 is a radius of point defect. By this way it is clear

that the electric field necessary to make stress can be evaluated as following: $E = \frac{4\alpha\pi r_0^3}{3Ze}(\sigma_{11} + \sigma_{22} + \sigma_{33})$.

8. MGT model and mechanism of crystal phase destruction by local fields

$$F_i = \frac{1}{2} \sum_j N_j (E_j - e\vec{E}_j \cdot \vec{x}_j)$$

Free energy is determined as energy E_j per one bond, N_j is a quantity of neighbor atoms, \vec{E}_j is electric field, and vector \vec{x}_j of dipole that is due to the inter atomic bond, such as Si-O, for example. Inter atomic bond length (for Si-O bond) can be calculated by using the following formula proposed by S. Hasegawa and co-workers [29] $d_{SiO} = d_{SiO}^{nonpolar} - B_{Si}\delta q_{Si} - B_O\delta q_O$, where δq_{Si} and δq_O are partial charges for atoms, and B_{Si} and B_O are empirical factor that has its positive value. Therefore, for different directions is

$$\frac{F_1}{F_2} = \sum_1 N_1 \left(\frac{E_1 - \delta Q_1 E \rightarrow_1 x_1 \rightarrow}{\sum_2 N_2 (E_2 - \delta Q_2 E \rightarrow_2 x_2 \rightarrow)} \right); \quad (21)$$

For estimation the ratio between the energy of deformation and weak bond length which can be appeared by applying the external electric field we can use the Einstein relation for relation between the drift velocity and applying force $v_{drift} = \frac{D}{kT} F \cdot \frac{\vec{\mu}}{d} = \frac{kT}{D} vN$; where N is quantity of atoms that was locations were deformed, d is bond length of polarized silicon. The N value can be evaluated as following $N = \frac{D}{kTv} \frac{\vec{\mu}}{d}$. Here D is a diffusion coefficient, T is temperature, $\mu \rightarrow$ is a dipole moment of bond. The model of kinetic behavior of densities of dangling bonds and weak bonds which are generated by local electric field can be described by using the following

$$\begin{aligned} \frac{dN_{DB}}{dt} &= -W_1(N_{DB} - N_{WB}) - W_2(N_{DB} - N_H) \\ \frac{dN_{WB}}{dt} &= W_1(N_{DB} - N_{WB}) - W_3(N_{WB} - N_{FB}); \end{aligned} \quad (22)$$

where N_H is the density of silicon-hydrogen bonds, N_{DB} is the density of dangling bonds, and N_{WB} is a density of weak bonds, W_1 is a rate of dangling bonds elimination and weak bonds creation due to the annealing of silicon, mainly, but the W_2 is a rate of generating of dangling bonds due to the hydrogen diffusion, W_3 is a rate of floating bonds generating due to the decreasing of density of weak bonds. It is assumed, that the values W_2 and W_3 are the same order of magnitude. For atomic diffusion coefficient the following formula is $D = D_0 \exp\left(-\frac{E_A}{kT}\right)$; where E_A is activation energy value and theoretical equation for D_0 can be written as

follows $D_0 = n\alpha \exp\left(\frac{\Delta S}{k\nu a^2}\right)$ [30]; where n is a number of neighbor interstitial places of location, ν is frequency of vibrations in interstitial position, a is a lattice constant, α is a coefficient that value depends on the interstitial position, ΔS is an entropy $\Delta S = -\frac{\partial \Delta F}{\partial T}$, ΔF difference in free energy that equals to the energy of activation. However, the total fraction of neutral interstitial is low compare with density of bulk atoms and according to W. Harrison studying [31], their number is approximately 10^{14} cm^{-3} by the melting temperature. Therefore, the diffusion as interstitial as dopant diffusion plays mainly if we observe only the hydrogen diffusion with

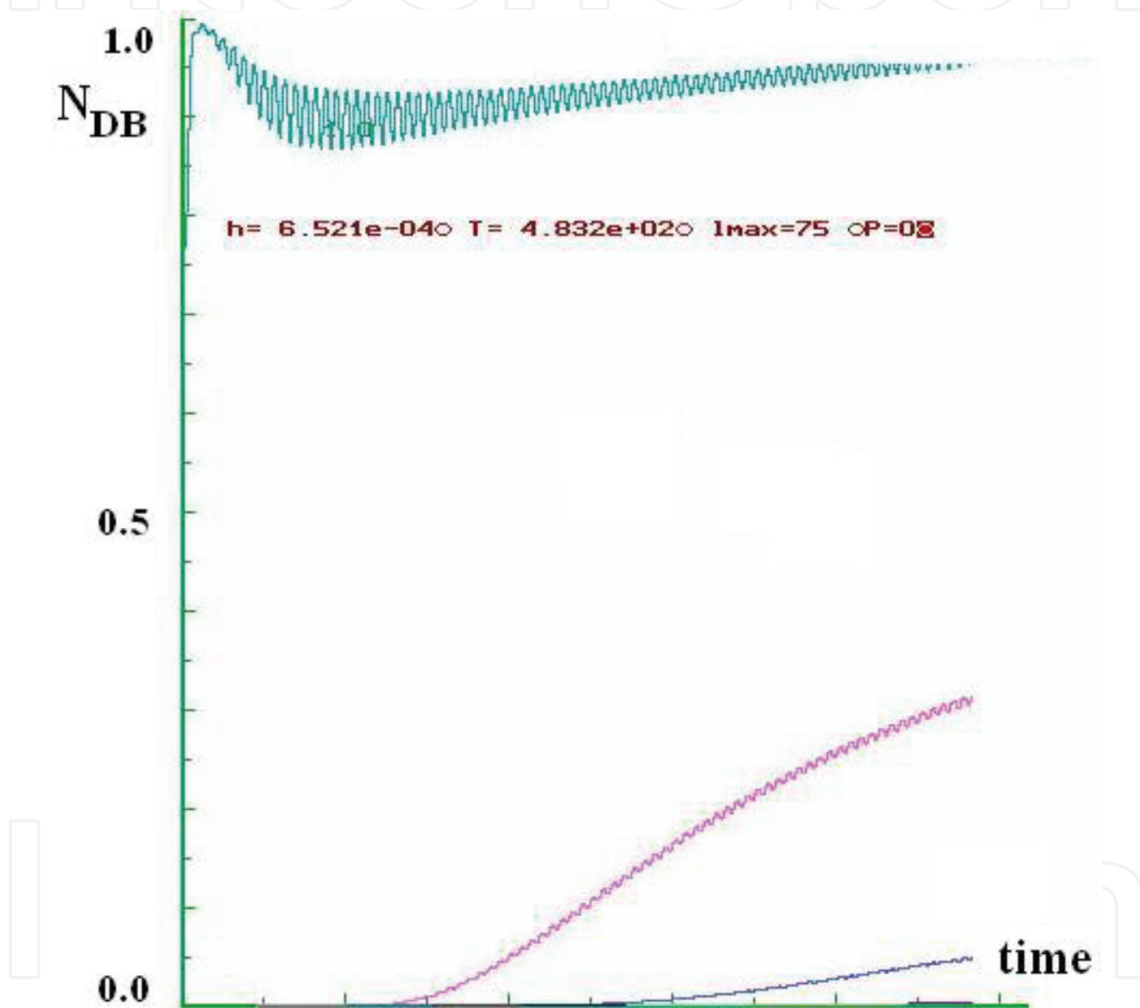


Figure 13. Evolution of density of dangling and weak bonds for different degrees of atomic sites order apart from the central of local electric field. It is assumed, that the values are $W_2 = W_3$. It is seen, that there is a reconstruction of the order by initial increasing of weak bond density, and redistribution of particles' local places according to the surrounding density values. It is assumed that this is a creation of order of amorphous phase. The third curve illustrates the evolution of density of perturbed bonds of next degree of order from the distance of a local electric field center. Oscillations of density of dangling bonds reflect the reconstruction of bonds and destruction by the annealing, hydrogen migration, according to the initial order of fixed atomic places of crystal structure and their new amorphous local placing. Over the period of time T the oscillations are suppressed by redistribution of initial impulse created by local field center and caused the increasing of weak bond density value. By this way the deformation penetrates in the surrounding of local area that will be larger than before.

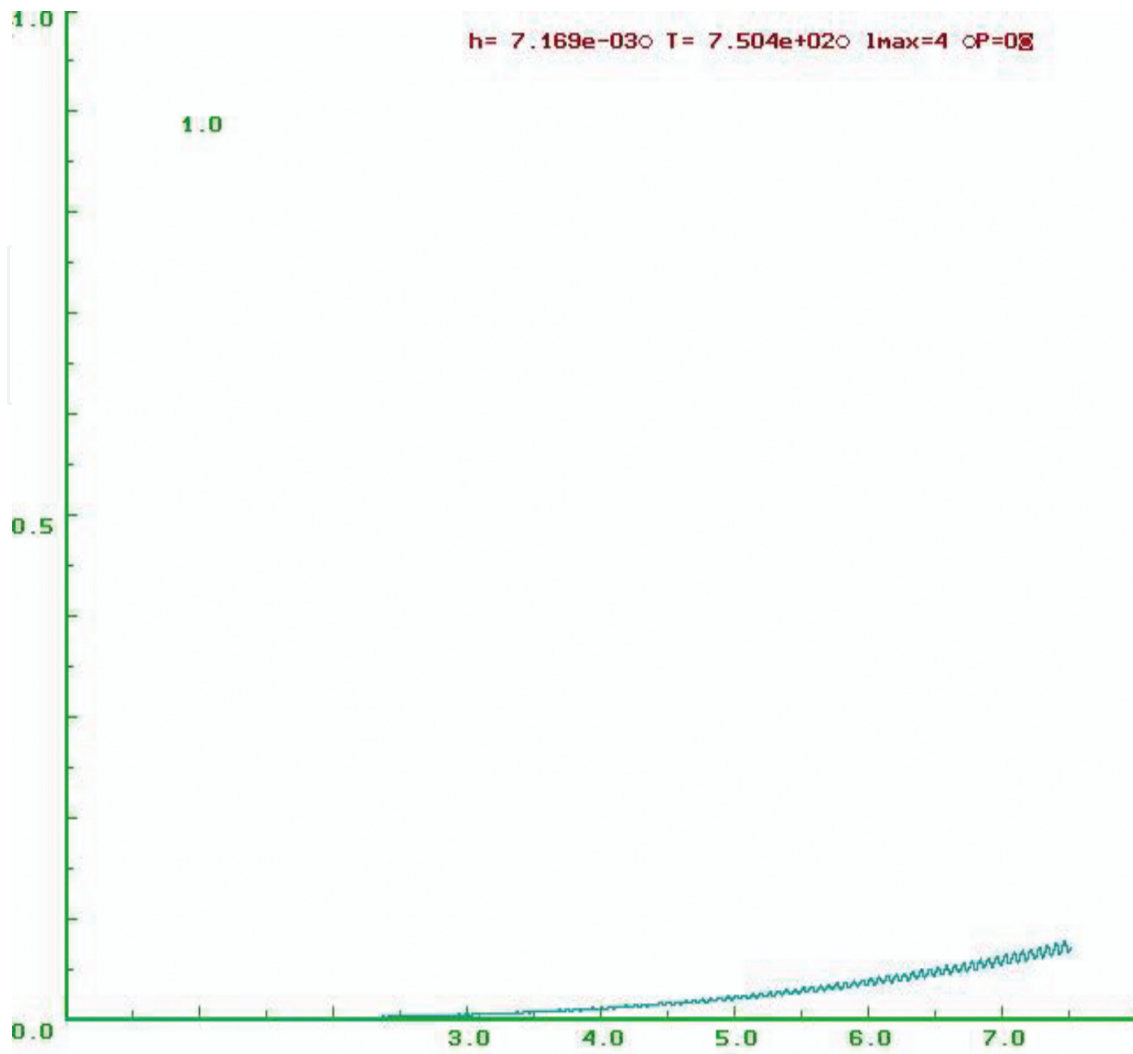


Figure 14. Evolution of density of dangling bonds for different degrees of atomic sites order apart from the central of local electric field, by the ratio between the values $W_2 = 0.001 \cdot W_3$. This scenario can describe the poor hydrogen contamination of silicon network.

energy of its activation 1.5 eV [32] and investigate the hydrogen moving through the sites with different potential caused by variation in electric charges.

Analytical solution of system of differential equations results in the following expression for density of dangling bonds

$$N_{DB} = N_{DB}^{(0)} \exp\left(-\frac{A}{2}t\right) \left[\exp\left(\sqrt{\frac{A^2}{4} - B}\right)t + \exp\left(-\sqrt{\frac{A^2}{4} - B}\right)t \right] - \frac{C}{B}; \text{ where the values are given.}$$

$A = W_2 + 2W_1 + W_3$; $B = W_2(W_1 + W_3) - W_1W_3$; $C = (W_1 + W_3)W_1N_H + W_1W_3N_{FB}$. By the relation between values W_2 and W_3 as $W_2 = 0.001 \cdot W_3$, or $W_2 \rightarrow 0$, the coefficients A , B , C have view.

$A_{W_2=0} = 2W_1 + W_3$; $B_{W_2=0} = -W_1W_3$; $C_{W_2=0} = (W_1 + W_3)W_1N_H + W_1W_3N_{FB}$ and the solution in this case can be written as.

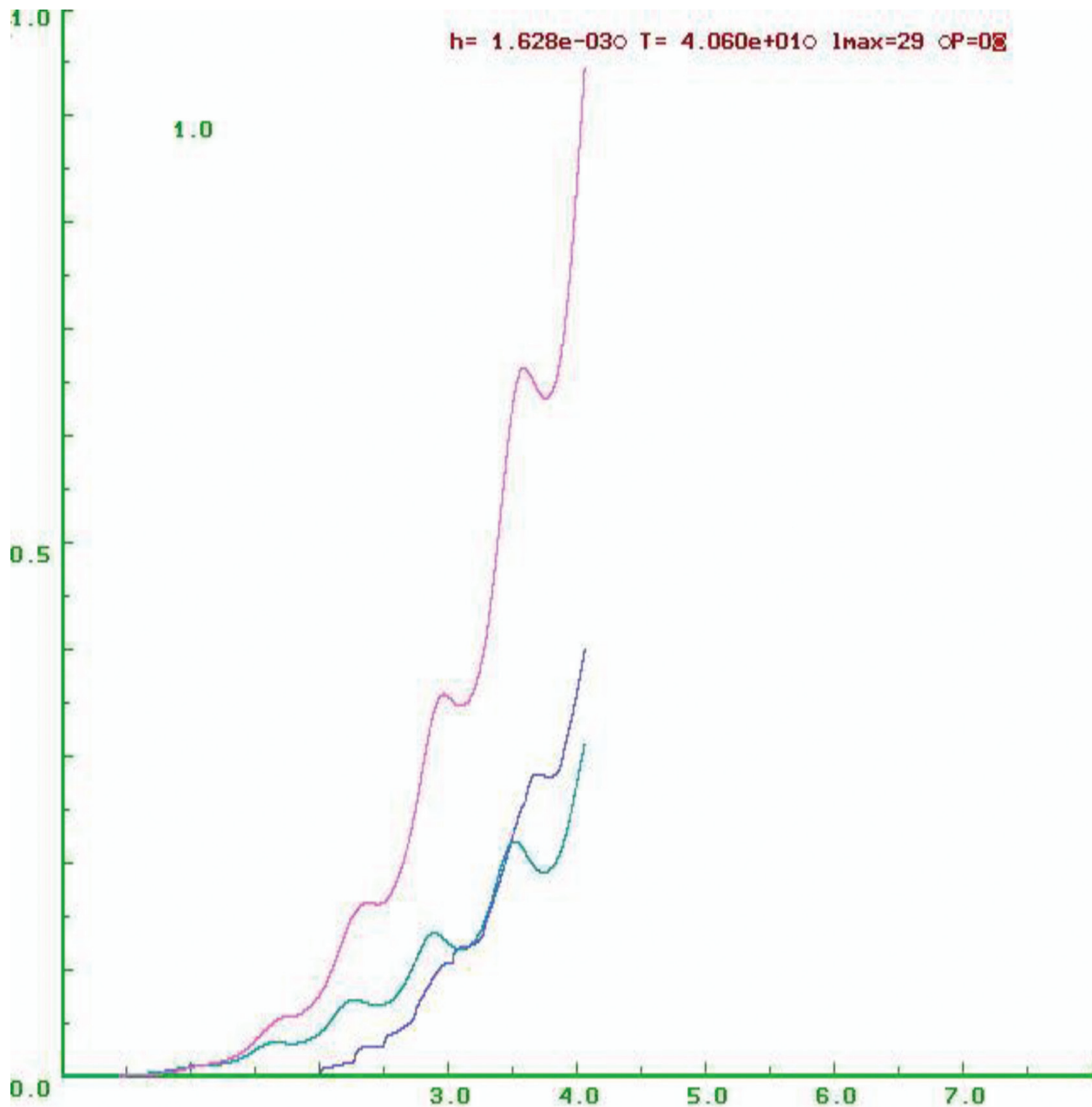


Figure 15. Evolution of density of dangling bonds for different degrees of atomic sites order apart from the central of local electric field, by the ratio between the values $W_2 = 0.01 \cdot W_3$. It is clear, that there is amorphization of the solid because the atomic sites order was damaged. It is assumed that such scenario can be explained the difference in quantity of dangling bonds near the local field center N_{DB}^{Local} and surrounding, $N_{WB}^{Surrounding}$, $N_{WB}^{Surrounding} > N_{DB}^{Local}$. The conservation law can explain that the small number of particles which are placed near local field center cause the changes in impulses of numerous atoms in surrounding area.

$$N_{W2=0} = N_{W2=0}^{(0)} \exp \left[\sqrt{W_1^2 + \frac{W_3^2}{4}} - W_1 - \frac{1}{2} W_3 \right] t^* \left[1 + \exp \left(-\sqrt{4W_1^2 + W_3^2} \right) t \right] + \frac{(W_1 + W_3)}{W_3}$$

$N_H + N_{FB}$; where $W_1 > W_3/3$ should be realized for increasing the density of dangling bonds, and in this case the density of dangling bonds has a slow rising over the time (as it is shown in **Figure 13**). By using the Runge–Kutta method of 4-th order it is easy to calculate the evolution

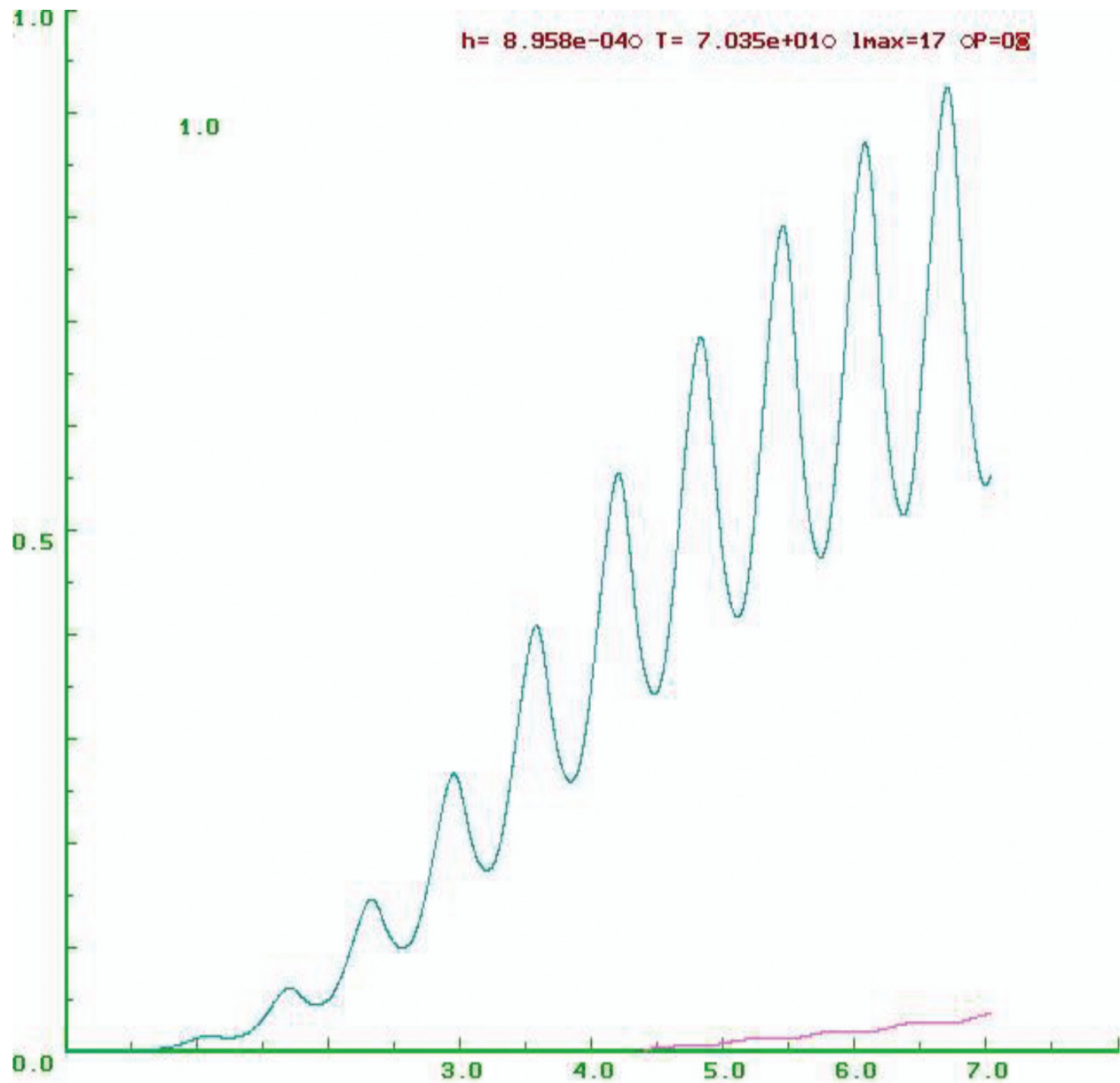


Figure 16. Evolution of density of dangling bonds for different degrees of atomic sites order apart from the central of local electric field, by the ratio between the values $W_2 = 0.1 \cdot W_3$.

of density of dangling bonds by the local electric field in several regimes for $N_{DB}(t)$, $N_{WB}(t)$ as normalized values of density of dangling and weak bonds.

It is known the model of defects generating by light irradiation in amorphous silicon which was proposed by the scientists of Ames Laboratory [33] which calculated the evolution of density of dangling bonds according to their proposed model. It is seen, that the evolution which was shown in **Figure 14** has the same increasing tendency as evolution stimulated by light irradiation. By the values $W_2=0.001 \cdot W_3$ the evolution changes its sharp increasing to the slow behavior of density of dangling bonds function as it is seen in **Figure 14**.

By the ratio between rates W_2 and W_3 equals to 100 the calculating evolution of density of dangling bonds can be presented as that was shown in **Figure 15**.

By the ratio between rates W_2 and W_3 equals to 10 the calculating evolution of density of dangling bonds can be presented as that was shown in **Figure 16**.

Author details

Dmitry E. Milovzorov

Address all correspondence to: dmilovzorov2002@yahoo.com

Fluens Technology Group, Ltd., Moscow, Russia

References

- [1] Maxwell-Garnett JC. Colors in metal glasses and metallic films. Philosophical Transactions. Royal Society of London. 1904;**203**:385. ISSN 1364-503X
- [2] Lorentz HAW. Annalen. 1880;**9**:641. ISSN 0003-3804
- [3] Brugeman DAG. Annalen der Physik. Leipzig. 1935;**24**:638
- [4] Stoner E. Demagnetizing factor for ellipsoids. Philosophical Magazine. 1945;**36**:263. ISSN 1478-6435
- [5] Osborn J. Demagnetizing factor of the general ellipsoid. Physical Review. 1945;**67**:351. ISSN 0163-1829
- [6] Ishiguro M, Ueno M. Observation Studies of Interplanetary Dust, Lecture Notes in Physics. Nakamura, Mukai, Springer: Mann; February 2009
- [7] Sankrit R, Blair W, Raymond J, Williams B. Dust destruction in the Cygnus Loop supernova remnant, Supernova Environmental Impact, Proceedings IAU Symposium No 296, 2013, eds. A. Ray and R. McGray
- [8] Mann I, Czechovsky A. Dust destruction and ion formation in the inner solar system. The Astronomical Journal. 2005. ISSN 0004-6256
- [9] Raymond P, Chavamian B, Williams W, Blair K, Borkovsky T, Gaetz R, Sankrit. Grain destruction in a supernova remnant shock wave. The Astrophysical Journal of AAS. 2013; **778**:161. 9 pp. ISSN 0004-6256
- [10] Landi S, Meyer-Vernet N, Zaslavsky A. On the Unconstrained Expansion of a Spherical Plasma Cloud Turning Collisionless: Case of Cloud Generated by a Nanometer Dusty

Grain Impact on an Uncharged Target in Space, Plasma Physics and Controlled Fusion, April 2012, arXiv.1205.1718v.1, publication No 241779851. ISSN 0741-3335

- [11] Milovzorov D. Point defects in amorphous and nanocrystalline fluorinated silicon. Journal of Materials Science and Engineering with Advanced Technology. 2010;**2**:41-59. ISSN 0976-1446. ISSN 0976-1446
- [12] Stockman, M. Local fields' localization and Chaos and nonlinear-optical enhancement in clusters and composites, in Optics of Nanostructured Materials, ed. by V. Markel, T George, John Wiley & Sons, 313–343 (2001)
- [13] Zimbovskaya N, Gumbs G. Long-range electron transfer and electronic transport through the macromolecules. Applied Physics Letters. 2002;**81**:1518-1520. ISSN 0003-6951
- [14] Compaan A, Trodahl HJ. Physical Review B. 1984;**29**:793. ISSN 0163-1829
- [15] Richter H, Wang Z, Ley L. The one phonon Raman spectrum in microcrystalline silicon. Solid State Communications. 1981;**39**:625. ISSN 0038-1098
- [16] Wright O. Thickness and sound velocity measurement in thin transparent films with laser picoseconds acoustics. Journal of Applied Physics. 1992;**71**:1617-1627. ISSN 0021-8979
- [17] Weinreich G, Sanders T, White H. Acoustoelectric effect in n-type germanium. Physical Review. 1959;**114**:33-44. ISSN 0163-1829
- [18] Geissberger AE, Galeener FL. Raman studies of vitreous SiO₂ versus fictive temperature. Physical Review B. 1983;**28**:3266-3271. ISSN 0163-1829
- [19] Raldugin VI. Physico-chemistry of surface. Dolgoprudny. 2011;**568**. (on Russian). ISBN 978-5-91559-116-4
- [20] Abtew TA, Drabold DA. Light-induced structural changes in hydrogenated amorphous silicon. Journal of Optoelectronics and Advanced Materials. 2006;**8**:1979-1988. ISSN 1454-4164
- [21] Milovzorov D. Acoustoelectric effect in microcrystalline and nanocrystalline silicon films prepared by CVD at low and high deposition temperatures. Journal of Physics. 2012;**1**:38-49. ISSN 0953-4075
- [22] Stewart GW, Sun J. Matrix Perturbation Theory. San Diego: Academic Press; 1990. p. 189 ISBN 0-12-670230-6
- [23] Lakno V. Clusters in physics, chemistry, biology. Izhevsk. 2001;**256**. (on Russian)
- [24] Britton D, Harting M. The influence of strain on point defect dynamics. Advanced Engineering Materials. 2002;**4**:629-633. ISSN 1438-1656
- [25] Emin D. Energy spectrum of an electron in a periodic deformable lattice. Physical Review Letters. 1972;**28**:804-807. ISSN 0163-1829
- [26] Milovzorov D. Crystalline phase destruction in silicon films by applied external electrical field and detected by using the laser spectroscopy. In: Huffaker DL, Eisele H, Dick KA,

editors. Quantum Dots and Nanostructures: Growth, Characterization, and Modeling XIII Edited. Vol. 9758. SPIE Proceedings; 2016. p. 11. DOI: 10.1117/12.2208270

- [27] Hausdorff F. Grundzuge der Mengenlehre. Vol. 184. Berlin; 1914 3-540-42224-2
- [28] Landau L, Lifshitz E. Elastic Theory. Moscow; 1987. pp. 51-56 (on Russian). ISBN 978-0-7506-2633-0
- [29] Hasegawa S, He L, Amano Y, Inokuma I. Physical Review B. 1993;**48**:5315. ISSN 0163-1829
- [30] Wert C, Zener C. Interstitial atomic diffusion coefficient. Physical Review. 1949;**76**:1169-1175. ISSN 0163-1829
- [31] Harrison W. Diffusion and carrier recombination by interstitials in silicon. Physical Review B. 1998;**57**:9727-9735. ISSN 0163-1829
- [32] Powel M, Dean S. Microscopic mechanism for creation and removal of metastable dangling bonds in hydrogenated amorphous silicon. Physical Review B. 2002;**66**:155212. ISSN 0163-1829
- [33] Biswas R, Pan B, Ye Y. Metastability of amorphous silicon from silicon network rebonding. Physical Review Letters. 2002;**88**:205502. ISSN 0163-1829

IntechOpen

